  Bull. Chem. Soc. Jpn., 65, 3122—3134 (1992) [Vol. 65, No. 11

Theoretical Study of Structure and Thermodynamic Properties of Liquid Hydrogen Fluoride

Kazuhiko HONDA,† Kazuo KITAURA, and Kichisuke NISHIMOTO*,††
Institute for Molecular Science, Myodaiji, Okazaki 444
†† Department of Chemistry, Osaka City University, Sumiyoshi-ku, Osaka 558
(Received July 10, 1992)

Monte Carlo (MC) simulations for liquid hydrogen fluoride (HF) were carried out using a new type of intermolecular potential function. The bonding energy distribution function was found to have three peaks corresponding to the distributions of molecules which have one, two, and three hydrogen bonds with neighbors. A partition function of liquid HF was derived referring to the results of MC simulations, where a simple Hamiltonian consisting of harmonic oscillators and hydrogen bond energies was employed. The thermodynamic properties calculated by the partition function reasonably reproduced the experimental data. Moreover, the effects of hydrogen bondings on various thermodynamic properties were revealed based on the partition function.

Liquid HF is one of the interesting substances used to study the effects of hydrogen bonding on structures and thermodynamic properties. HF molecules can form hydrogen bonds as strong as the water dimer in the gas phase.[1] However, unlike liquid water, the anomaly of the thermodynamic properties of liquid HF is not recognized, except for the large isothermal compressibility.[2] The purposes of this work were as follows:

1. Elucidation of the unique structure of liquid HF by Monte Carlo (MC) simulations using a new type of intermolecular potential function generated by ab initio intermolecular interaction energies.
2. Elucidation of hydrogen bonding effects on thermodynamic properties of liquid HF using a partition function which is constructed by a simple model involving the results of MC simulations.

Several MC and molecular dynamics simulations have been carried out for liquid HF.[3-6] The calculated statistical properties greatly depended on the intermolecular potential functions used in the simulations. For instance, in some studies[3,6] an F–F radial distribution function having a shoulder in the first peak was obtained. However, in other studies[4,5] it had no shoulder. The potential functions used in the previous work were the so-called atom–atom type potentials. They may be difficult to represent intermolecular potentials accurately for molecules having lone pair electrons. For such molecules,[5,7,8] atom–atom type potentials require additional virtual interaction sites located at physically unreasonable places. For example, in H_2O it is located at opposite to the lone pairs.[8] For HF molecules, one can introduce interaction sites only on the axis along the HF bond, since the molecular symmetry of $C_{\infty v}$ should be maintained. This restriction, however, results in difficulties to obtain an accurate atom–atom type potential for (HF)···(HF).

In the present study we used a new type of intermolecular potential function[9] which is expressed in terms of the overlap integrals over localized orbitals of the molecules. Our potential function may be called a bond–bond type potential, which reasonably well reproduces the interaction energies calculated by the ab initio MO method without introducing any artifical interaction sites, even for molecules which have lone pair electrons.

Since the potential function is derived based on molecular orbital theory for intermolecular interactions,[10] it takes the quantum mechanical effects into accounts to some extent.

The MC simulations of liquid HF were performed using our potential function. The first peak of the F–F radial distribution function does not have any shoulders, compared with the Jorgensen's result,[4,5] but not with Klein's.[3,6] The bonding energy distribution function, however, is quite different from that of Jorgensen's. We obtained a bonding energy distribution function with two shoulders at both sides of the main peak, which was not found in previous work. This result suggests that there are three different environments of molecules in liquid HF, which correspond to molecules having one, two and three hydrogen bonds with neighbors, respectively. Such a multiplet is supposed by the mixture model of liquid water.[11] However, as far as we know, it has been found only for liquid alcohols.[12] Our result is only the second case of such a multiplet.

In order to elucidate the thermodynamic properties of liquid HF, we derived a partition function while referring to the results of MC simulations, and evaluated various thermodynamic properties. The effects of hydrogen bondings on the various thermodynamic properties were analyzed using the partition function, and comparisons were made between liquid HF and liquid water.

Potential Function

The intermolecular potential function for (HF)···(HF) is expressed as follows:

$$V_{\mathrm{HF,HF}} = C_{\mathrm{HF\,HF}} S_{ij}^2 + C_{\mathrm{HF}\,\sigma\mathrm{L}} \sum_{\substack{i\in\mathrm{HF}\\ l\in\sigma\mathrm{L}}} S_{il}^2 + C_{\mathrm{HF}\,\pi\mathrm{L}} \sum_{\substack{i\in\mathrm{HF}\\ m\in\pi\mathrm{L}}} S_{im}^2 + C_{\sigma\mathrm{L}\,\sigma\mathrm{L}} S_{\sigma\mathrm{L}\,\sigma\mathrm{L}}^2 + C_{\sigma\mathrm{L}\,\pi\mathrm{L}} \sum_{\substack{k\in\pi\mathrm{L}\\ m\in\pi\mathrm{L}}} S_{km}^2 + C_{\pi\mathrm{L}\,\pi\mathrm{L}} S_{\pi\mathrm{L}\,\pi\mathrm{L}}^2$$

† Present address: Toyohashi University of Technology, Tempaku-cho, Toyohashi 441.

$$+ C'_{HF^*HF} \sum_{\substack{i^* \in HF \\ j \in HF}} S^2_{i^*j} + C'_{HF^*\sigma L} \sum_{\substack{i^* \in HF \\ l \in \sigma L}} S^2_{i^*l} + C'_{HF^*\pi L} \sum_{\substack{i^* \in HF \\ m \in \pi L}} S^2_{i^*m} + \sum \frac{Q_r Q_s}{R_{rs}}. \quad (1)$$

A HF molecule has five localized orbitals:[13] H–F bonding (HF), H–F antibonding (HF*), σ lone pair (σL), and two π lone pair (πL) orbitals. S_{ij} in Eq. 1 refers to the intermolecular overlap integral associated with localized orbitals, i and j. C_{AB} is the parameter for a given bond-bond pair, which is determined so as to reproduce *ab initio* interaction energies. The last term is the Coulomb interaction between molecules, which comprises electrostatic interactions between fractional point charges (Q_r) on atom r in molecule A and Q_s on atom s in molecule B. R_{rs} is the internuclear distance between atoms r and s. Details concerning the potential function are referred to in our previous paper.[9]

The energies of the generated potential function are compared with the *ab initio* interaction energies at various intermolecular distance and various mutual orientations of the dimer (Fig. 1). The potential energy curves along some geometrical parameters are also shown in Fig. 2. As can be seen from these figures, our potential function describes reasonably well the orientational dependencies of the interactions between the hydrogen bonding molecules without introducing any artificial interaction sites.

The optimized geometries of the HF dimers are shown in Fig. 3. The linear configuration is an energy minimum, while the cyclic configuration is not. The cyclic dimer is obtained by optimizing only the geometrical parameters of r and θ. The calculated F–F distance of the linear dimer is shorter than that of the experiment. This is due to the poor STO-3G basis set used in calculating the *ab initio* interaction energies to generate the potential function. The calculated hydrogen bond energy (23.8 kJ mol^{-1}) is accidentally almost equal to the experimental energy (20.9±6.3 kJ mol^{-1} [15]). The several optimized geometries of the trimers and the tetramers are also shown in Figs. 4 and 5, respectively. The geom-

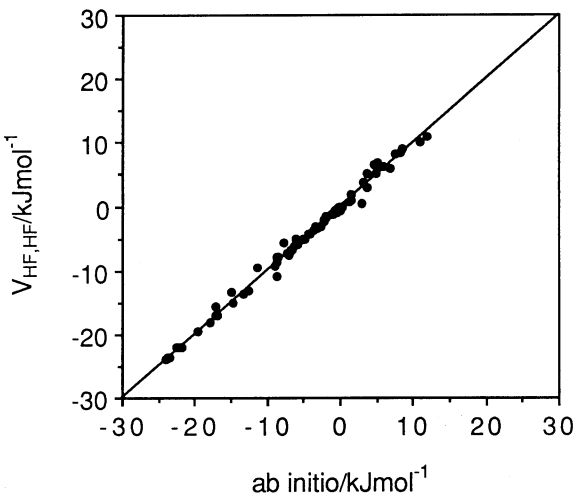

Fig. 1. Comparisons of the interaction energies of the HF dimers from ab initio STO-3G calculations and the potential energy function, $V_{HF,HF}$, at the sampled dimer configurations.

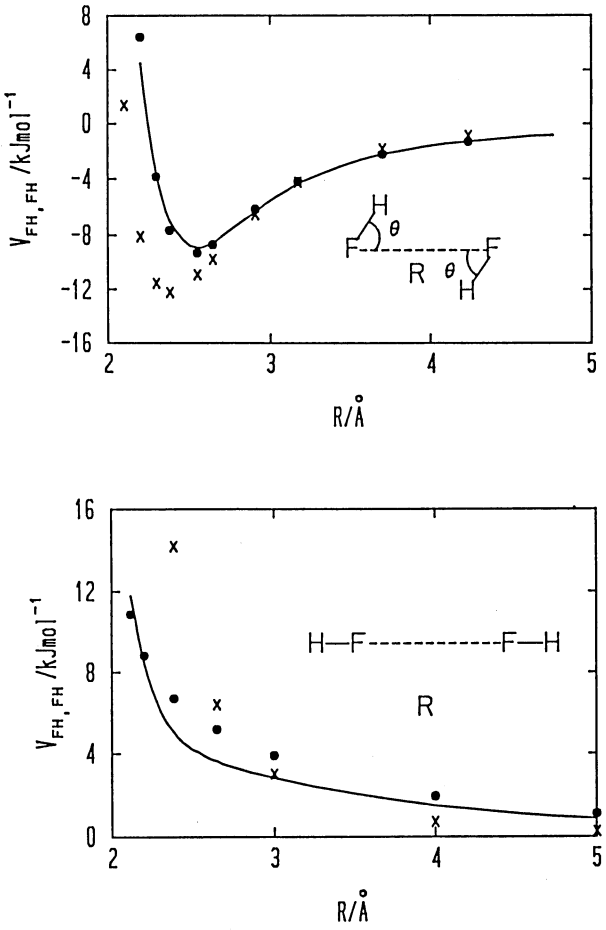

Fig. 2. Potential energy curves for the HF dimers. —: *ab initio* STO-3G, ●: potential function of this work, ×: Jorgensen's potential function. (Ref. 5), θ=58°.

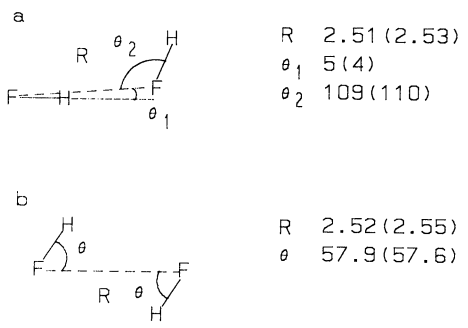

Fig. 3. Optimized geometries of HF dimers. R in Å and θ in degrees. In the parenthesis are given the ab initio STO-3G calculations. The experimental geometrical parameters of linear dimer are 2.79 Å and 115° for R and θ (Ref. 14), respectively.

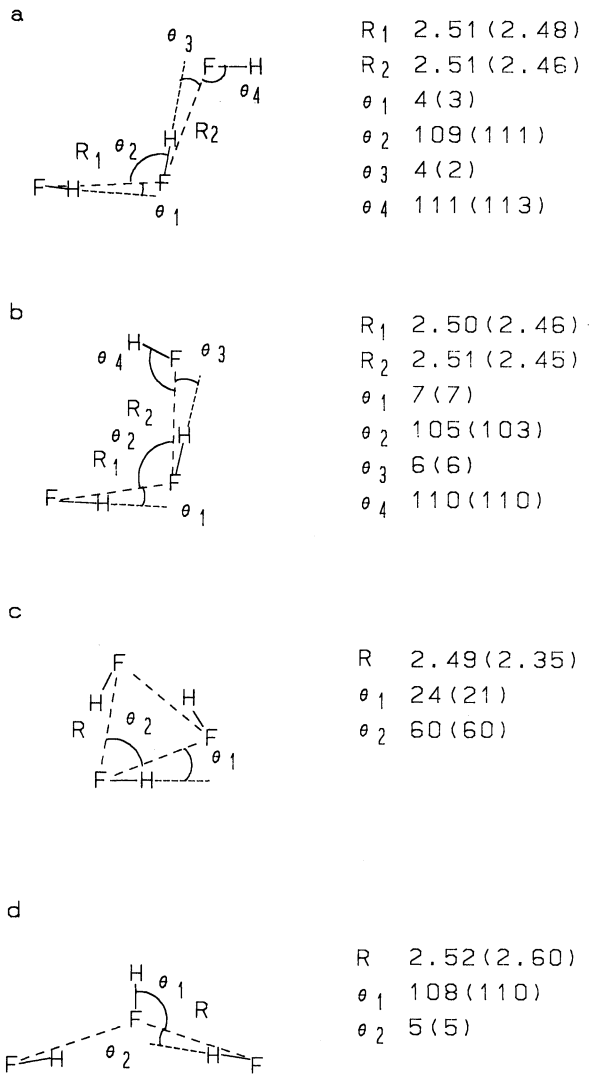

Fig. 4. Optimized geometries of trimers. R in Å and θ in degrees. The molecules lie on a plane for all geometries. The point group symmetries of c and d are C_{3h} and C_{2v}, respectively.

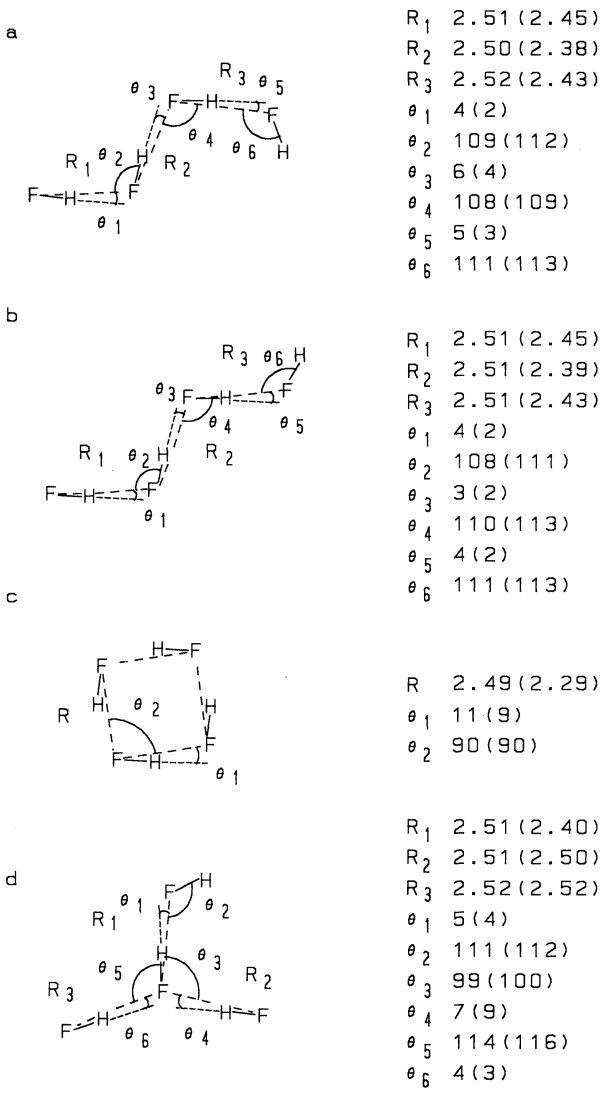

Fig. 5. Optimized geometries of tetramers. R in Å and θ in degrees. The point group symmetry of c is C_{4h}.

etries obtained from our potential function agree satisfactorily with those from the *ab initio* MO calculations.

MC Simulations

The MC simulations were performed on liquid HF in the standard manner using the periodic boundary condition and the Metropolis sampling algorithm[16,17] for 125 molecules in the base cell using the potential function discussed in the previous section. The first 10 K steps were discarded and the successive 30 K steps were used for statistical averaging (a step means 125 random trials).

A drawback of our potential function is that it consumes much computer time to calculate the overlap integrals. A speed-up is possible by using tables of overlap integrals for atomic pairs; it is prepared at the beginning of an MC run. Computational details concerning overlap integral calculations were described in a previous paper.[18]

Results and Discussion

Distribution Function. The radial distribution functions at a temperature of 273 K and a density of 1.0 g cm^{-3} are shown in Fig. 6. No experimental data are available. Our results compare with those of Jorgensen's.[5] The locations of the first peaks of the distribution functions roughly correspond to the interatomic distances of the linear HF dimer shown in Fig. 3. Taking this and the broad second peaks into account, we consider that the structure of liquid HF comprises flexible chains of hydrogen bonded molecules.[5,6] It has been suggested that interactions between chains cause a shoulder at the first peak of the F–F radial distribution function.[3,6] However, in our result, there is no shoulder

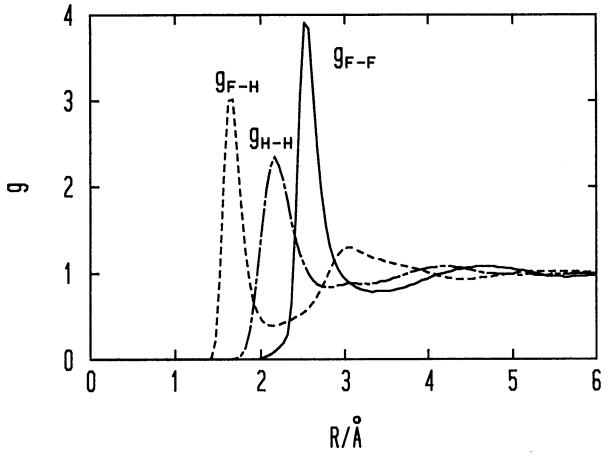

Fig. 6. Radial distribution functions of liquid HF at the temperature of 273 K and the density of 1.0 g cm^{-3}.

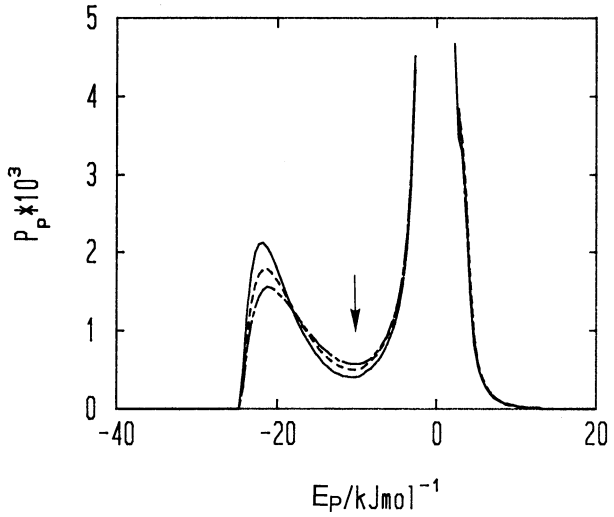

Fig. 7. Temperature dependence of pair energy distribution functions at a density of 1.0 g cm^{-3}. —: 273 K, ----: 300 K, –·–·–: 325 K. The arrow indicates the pair energy threshold (see text).

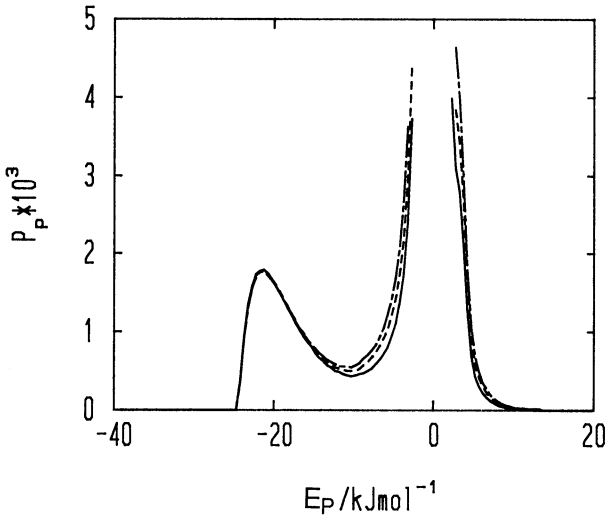

Fig. 8. Density dependence of pair energy distribution functions at a temperature of 273 K. —: 0.8 g cm^{-3}, ----: 1.0 g cm^{-3}, –·–·–: 1.2 g cm^{-3}.

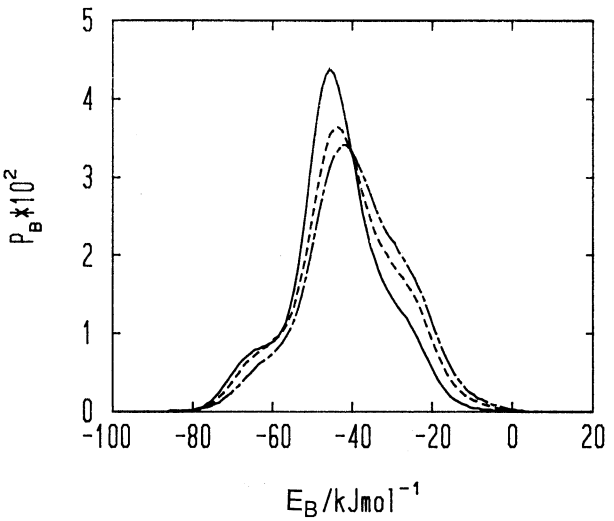

Fig. 9. Temperature dependence of bonding energy distribution functions at a density of 1.0 g cm^{-3}. —: 273 K, ----: 300 K, –·–·–: 325 K.

in the first peak. It would be desirable to examine whether the first peak has a shoulder or not for real liquid HF by using a more sophisticated potential function.

Figure 7 shows the pair energy distribution functions at various temperatures and at a density of 1.0 g cm^{-1}. The peak of the distribution function is located at an energy of about −20.0 kJ mol^{-1}. The distributions around the peak correspond to the hydrogen bonded molecules. As can be seen in Fig. 7, with an increase in the temperature the height of the peak becomes lower, while that of the valley at an energy of about −10.0 kJ mol^{-1} becomes higher. This result suggests that the number of hydrogen bonds in the system decreases as the temperature rises. The density dependence of the distribution function is shown in Fig. 8. The distribution of non-bonded molecular pairs becomes broad as the density increases. However, the distributions corresponding to the hydrogen bonded pairs are almost unchanged. Thus, the number of hydrogen bonds slightly depends on the density of the liquid.

The bonding energy distribution functions at various temperatures and at various densities are shown in Figs. 9 and 10, respectively. There are two shoulders in the main peak of the distribution functions. This very interesting multiplet feature has not yet been obtained in the previous work on liquid HF. The multiplet of the bonding energy distribution function has been observed only for liquid alcohols.[12] The multiplet suggests that there are different environments of molecules in the liquid phase. In the following section we analyze the distribution function in detail from the viewpoint of the hydrogen bonding structures.

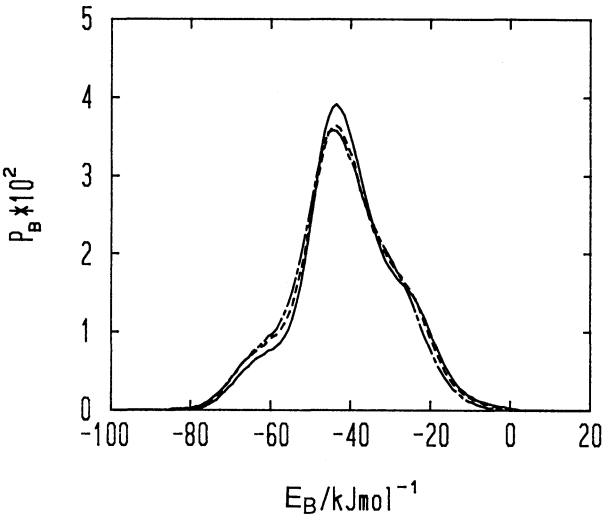

Fig. 10. Density dependence of bonding energy distribution functions at a temperature of 273 K. —: 0.8 g cm^{-3}, ----: 1.0 g cm^{-3}, -·-·-: 1.2 g cm^{-3}.

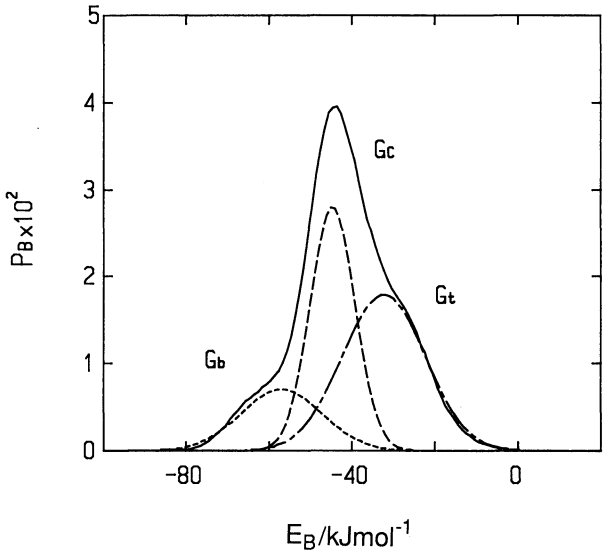

Fig. 11. Bonding energy distribution function decomposed into three Gaussian functions at a temperature of 273 K and a density of 1.0 g cm^{-3}. G_b: branch molecules. G_c: chain molecules, G_t: terminal molecules.

Hydrogen Bonding Structures. We decomposed the bonding energy distribution function into three Gaussian functions. The centers and exponents of the Gaussian functions were determined by a non-linear least-squares method under the normalization requirement of the distribution function (Fig. 11). The centers of the three Gaussians are at energies of −32, −45, and −57 kJ mol^{-1}, respectively. Among the molecules in the various configurations generated by the MC simulations, we picked up some typical molecules which have bonding energies corresponding to the three Gaussians, and found that they have one, two, and three hydrogen bonds with

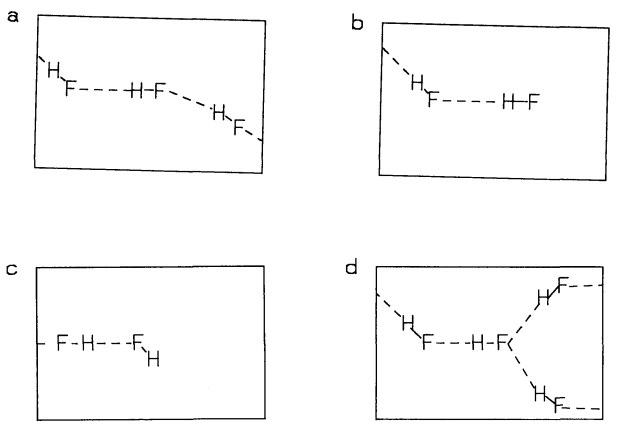

Fig. 12. Local hydrogen bond structures in liquid HF. a: chain, b: terminal ended with F atom, c: terminal ended with H atom, d: branched at F atom.

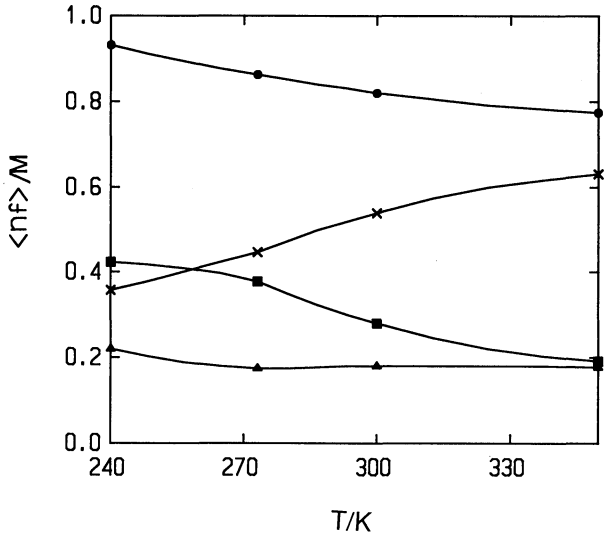

Fig. 13. Temperature dependence of the "molar fraction" of branch, ▲, chain, ■, and terminal, ×, molecules. The number of hydrogen bonds per molecule is indicated by ●.

neighbors, respectively, where the number of hydrogen bonds was counted using a threshold bonding energy of 10 kJ mol^{-1} between two molecules. The threshold energy was estimated referring to the pair energy distribution function (Fig. 7). There are only a few non-bonded molecules throughout the temperature range from 240 K to 350 K. A more detailed analysis of the hydrogen bonded structures revealed that there are four main local configurations, as shown in Fig. 12. The molecules having one, two and three hydrogen bonds with neighbors are hereafter referred to as the terminal, the chain and the branch molecules, respectively.

The 'molar fractions' of the terminal, the chain and the branch molecules were calculated from the three Gaussians (Fig. 13). The main species is a chain molecule. With an increase in the temperature, the popula-

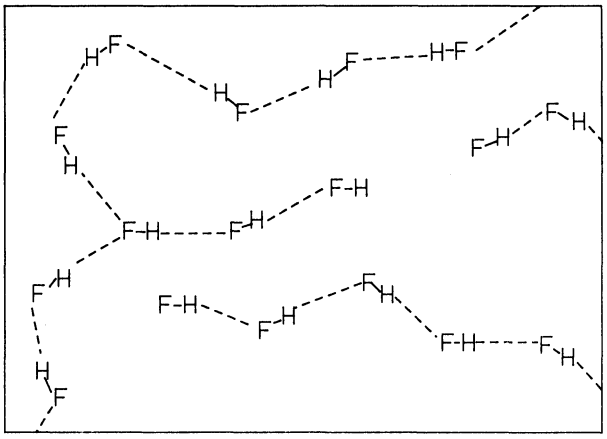

Fig. 14. Schematic representation of the structure of liquid HF.

tion of the chain molecules decreases and that of the terminal molecules increases, while the population of the branch molecules remains almost unchanged. From these facts, we can understand the structure of liquid HF as comprising chains of hydrogen bonded molecules with some branches. As the temperature rises, some hydrogen bonds are broken. This bond breaking occurs mainly at the chains, not at the branches. Hence, the chains become shorter at higher temperatures.

A schematic illustration of the structure of liquid HF is given in Fig. 14. There are zigzag hydrogen bonded chains aligned both parallel and antiparallel, depending on the type of holding and branching of chains. It is noted that we could not find molecules with two hydrogen bonds at the site of an H atom in the configurations generated by the MC simulations. This type of hydrogen bonded structure is energetically unfavorable. Actually, there is no corresponding stable structure of the HF trimers (Fig. 4). The hydrogen bonding structure of liquid HF reflects the structures of the dimers and trimers; especially, the modes of chain branching are restricted by the possible structures of the trimer (Fig. 12).

The total number of hydrogen bonds of the 125 molecules in the base cell is calculated by two different manners. One is to calculate from the bonding energy distribution function of the terminal, the chain, and the branch molecules described above. By integrating the Gaussian distribution functions and normalizing the total number of molecules to be 125, one obtains the number of terminal ($<n_t>$), chain ($<n_c>$) and branch ($<n_b>$) molecules. The total number of hydrogen bonds ($<n>$) is evaluated by

$$<n> = \frac{<n_t> + 2<n_c> + 3<n_b>}{2} \qquad (2)$$

since the terminal, the chain, and the branch molecules have one, two, and three hydrogen bonds, respectively. Another way is to count the number of hydrogen bonds directly in the MC simulation using a threshold bonding energy for the molecular pairs. The threshold energy employed was 10 kJ mol^{-1}, which was the same as the threshold energy used in an analysis of bonding energy distribution function. The total numbers of hydrogen bonds at 273 K and at a density of 1.0 g cm^{-3} were obtained to be 108 and 119 by the former and the later methods, respectively. They are comparable to each other, and our analyses of the bonding energy distribution function are rationalized.

Partition Function. i) Formulation: Various statistical models[11,19-22] have been proposed for liquid water in order to understand anomalous thermodynamic properties. The anomalous properties are due to the strong hydrogen bonds formed among water molecules in these models. The HF molecules can form strong hydrogen bonds as water molecules. The effects of the hydrogen bonds on the thermodynamic properties are also expected to be very important in liquid HF. No anomaly of the thermodynamic properties, however, has been observed for liquid HF, except for the large isothermal compressibility.[2] To elucidate the differences of the hydrogen bonding effects in these two liquids, we derive a partition function which allows us to calculate the thermodynamic properties and to analyze the hydrogen bonding effects on each thremodynamic property.

Let's assume that all of the local minima on a potential energy surface are known for M molecules in a base cell at a fixed volume. The potential energy (E) around the i-th local minimum may be expanded as

$$E(R_{ij};\, R_{i0}) = E(R_{i0}) + \frac{1}{2}\sum_{j}^{5M} k_{ij}(R_{ij} - R_{i0})^2, \qquad (3)$$

where $E(R_{i0})$ is the potential energy at the local minimum (R_{i0}), and the second term is a quadratic expansion of the potential energy along the normal coordinates (R_{ij}) around the minimum. The degree of freedom is $5M$ for the M HF molecules, since the rigid molecule approximation is employed. Therefore, R_{i0} and R_{ij} comprise $5M$ structural parameters. Using the approximation for the potential energy, the configurational partition function is evaluated as a sum of contributions from each local minimum:

$$Q(M, V, T) = \iint\cdots\int \exp\{-E(\boldsymbol{r}_1, \boldsymbol{r}_2, \cdots \boldsymbol{r}_M)/(k_BT)\}\mathrm{d}\boldsymbol{r}_1\mathrm{d}\boldsymbol{r}_2\cdots\mathrm{d}\boldsymbol{r}_M$$
$$= \sum_i \iint_{\Delta_i}\cdots\int \exp\{-E(\boldsymbol{R}_{ij};\, \boldsymbol{R}_{i0})/(k_BT)\}\mathrm{d}\boldsymbol{r}_1\mathrm{d}\boldsymbol{r}_2\cdots\mathrm{d}\boldsymbol{r}_M, \qquad (4)$$

where Δ_i is a subspace containing the i-th local minimum (Fig. 15). Actually, it is impossible to obtain all of local minimum configurations for a system comprising many molecules. It is therefore desirable to find a simple way to represent all of the possible minimum configurations of a system as well as their potential energies. We are following the approach referring to the results of the MC

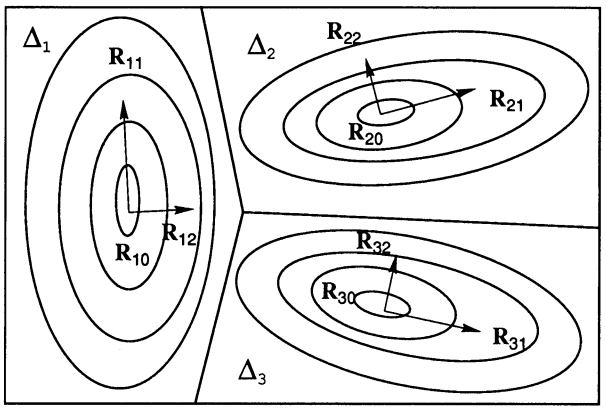

Fig. 15. Two-dimensional example of the quadratic expansion of the potential energy around local minima.

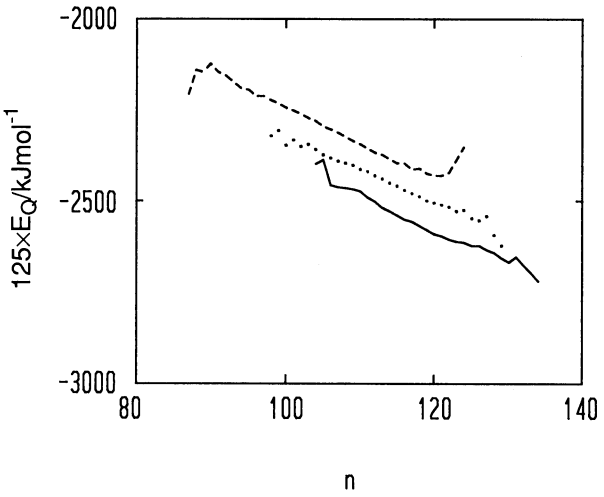

Fig. 16. Average configuration energy for a 125 molecular system plotted against the number of hydrogen bonds (n) at a density of 1.0 g cm^{-3}. —: 273 K, ----: 300 K, -·-·-: 325 K.

simulations.

The configuration energies obtained by the MC simulations were averaged over configurations whose number of hydrogen bonds were the same, where the numbers of hydrogen bonds were calculated using a threshold pair energy of -10 kJ mol^{-1}. Figure 16 shows that the configurational energies are linearly dependent on the number of hydrogen bonds (n) at a fixed temperature and density. The zigzags at both sides of the straight lines in Fig. 16 are due to statistical error, since the appearance probabilities are rather small in these energy regions. From the results, it is reasonable to assume that all of the possible configurations of an M molecular system are represented by index, n, and that their energies can be approximately written as a linear function of n. Thus, the potential energy around the i-th local minimum (Eq. 3) may be rewritten as

$$E(\boldsymbol{R}_{ij};\boldsymbol{R}_{i0}) = E_{\mathrm{H}}\cdot n_i + E_0 + \frac{1}{2}\sum_j^{5M} k_{ij}(\boldsymbol{R}_{ij}-\boldsymbol{R}_{i0})^2, \quad (5)$$

where E_{H} is the energy associated with one hydrogen bond and E_0 is the background potential energy, which does not depend on n.

Using the expression of the potential energy (Eq. 5), the configurational partition function (Eq. 4) becomes

$$Q(M,V,T) = \sum_i \Bigg[\exp\{-(E_{\mathrm{H}}\cdot n_i + E_0)/(k_BT)\} \times \iint_{\Delta_i}\cdots\int \exp\Big\{-\frac{1}{2}\sum_j^{5M} k_{ij}(\boldsymbol{R}_{ij}-\boldsymbol{R}_{i0})^2/(k_BT)\Big\}\mathrm{d}\boldsymbol{r}_1\mathrm{d}\boldsymbol{r}_2\cdots\mathrm{d}\boldsymbol{r}_M\Bigg]. \quad (6)$$

Here, we introduce further simplifications by assuming that the force constants in the third term of Eq. 5 do not depend on n but only on the volume of the system. In other words, the harmonic potentials are replaced by hypothetical harmonic potentials which are regarded as being averaged harmonic potentials for all configurations. Then, Eq. 6 becomes

$$\begin{aligned} Q(M,V,T) &= \Big[\sum_i \exp\{-(E_{\mathrm{H}}\cdot n_i + E_0)/(k_BT)\}\Big] \\ &\quad\times\Bigg[\iint_{\bar{\Delta}}\cdots\int \exp\Big\{-\frac{1}{2}\sum_j^{5M}\bar{k}_j\Delta\boldsymbol{R}_j^2/(k_BT)\Big\} \mathrm{d}(\Delta\boldsymbol{R}_1)\mathrm{d}(\Delta\boldsymbol{R}_2)\cdots\mathrm{d}(\Delta\boldsymbol{R}_{5M})\Bigg] \\ &= \Big[\sum_n g(n)\cdot\exp\{-(E_{\mathrm{H}}\cdot n_i + E_0)/(k_BT)\}\Big] \\ &\quad\times\Bigg[\prod_j^{5M}\int_{\bar{\Delta}}\exp\Big\{-\frac{1}{2}\bar{k}_j\Delta\boldsymbol{R}_j^2/(k_BT)\Big\}\mathrm{d}(\Delta\boldsymbol{R}_j)\Bigg], \end{aligned} \quad (7)$$

where $g(n)$ is the degeneracy or the density of states of the configurations which have n hydrogen bonds. $\bar{k}_j$ and $\bar{\Delta}$ are the averaged force constant and the averated integral region, respectively. We can not explicitly show just how averaged they are, but only conceptual ones.

To go further it would be necessary to estimate the density of state ($g(n)$). We assume that $g(n)$ is approximately represented by

$$\ln g(n) = a\cdot n^2 + b\cdot n, \quad (8)$$

where a and b are parameters which must be determined from the results of the MC simulations. The pertinence of this approximation should be certified. This is done later in the following section, where the distribution function of n is derived from the partition function; it is compared with that obtained directly from the MC simulations. Substituting Eq. 8 into Eq. 7 and replacing the sum over n with the corresponding integral, we obtain

$$Q(M, T, V)=\left[\int_0^{n_{\max}} \exp(an^2+bn)\cdot\exp\{(-(E_H\cdot n+E_0)/(k_BT)\}\mathrm{d}n\right] \times\left[\prod_j^{5M}\int_{\bar{\Delta}}\exp\left\{-\frac{1}{2}\bar{k}_j\Delta\boldsymbol{R}_j^2/(k_BT)\right\}\mathrm{d}(\Delta\boldsymbol{R}_j)\right], \quad (9)$$

where the integral over n is limited to $n_{\max}$, the maximum number of hydrogen bonds in an M molecular system. For liquid HF, $n_{\max}$ is assumed to be $2M/2$, since HF molecules have two hydrogen bonds in the crystal form.[23]

By combining the kinetic energy term together with the configuration partition function (Q) the total partition function (Z) can be written as

$$Z(M, T, V)=\int_0^{n_{\max}} \exp(an^2+bn)\cdot\exp\{(-(E_H\cdot n+E_0)/(k_BT)\}\mathrm{d}n \times\left[\prod_j^{5M}\int_P\int_{\bar{\Delta}}\exp\left\{-\left(\frac{P_j^2}{2m_j}+\frac{1}{2}\bar{k}_j\Delta\boldsymbol{R}_j^2\right)/(k_BT)\right\}\mathrm{d}(\Delta\boldsymbol{R}_j)\mathrm{d}P_i\right], \quad (10)$$

where p_j is the conjugate momentum and m_j is the reduced mass associated with the normal coordinate of $\boldsymbol{R}_j$. Although the range of integrals should be limited within a certain range of configuration space ($\bar{\Delta}$), for simplicity we expanded the range of the integral to all space, expecting that the actual contributions from the high-energy parts of the harmonic potentials would be small, at least in the range of the temperature of interest. Then, the second terms of Eq. 10 is nothing but the partition function of harmonic oscillators and the equation becomes

$$Z(M, T, V)=\int_0^{n_{\max}} \exp(an^2+bn)\cdot\exp\{(-(E_H\cdot n+E_0)/(k_BT)\}\mathrm{d}n \times\prod_j^{5M}\frac{1}{2\sinh\{h\nu_j/(2k_BT)\}} \quad (11)$$

The partition function comprises three terms (the hydrogen bond term (Z^H), the background potential term (Z^P) and the harmonic oscillator term (Z^O)):

$$Z^H(M, T, V)=\exp\left[-\frac{\{b-E_H/(k_BT)\}^2}{4a}\right]\times A(\chi),$$

$$Z^P(M, T, V)=\exp\{-E_0/(k_BT)\},$$

and

$$Z^O(M, T, V)=\prod_j^{5M}\frac{1}{2\sinh\{h\nu_j/(2k_BT)\}}, \quad (12)$$

where

$$A(\chi)=\int_\chi^{\chi+n_{\max}}\exp(at^2)\mathrm{d}t$$

and

$$\chi=\frac{b-E_H/(k_BT)}{2a}. \quad (13)$$

This feature of the partition function allows one to analyze the effects of the hydrogen bonds or contributions of the hydrogen bond term (Z^H) to the thermodynamic properties. This partition function is similar to that for liquid water,[18] which is derived based on different assumptions.

Until now, we assumed that M is the number of molecules in a base cell of the MC simulations. The partition function of N molecular system may be written as

$$Z(N, T, V)\propto\{Z^HZ^PZ^O\}^{N/M}, \quad (14)$$

where the proportional constant is not defined, since the absolute value of Z is not a matter of concern, though the expectation values of properties with respect to Z are. N is set to Avogadro's number in calculations of the thermodynamic properties.

ii) Determination of Parameters: The parameters involved in the partition function must be determined while referring to the results of the MC simulations.

First, we proceed to determine E_H and E_0. The configuration energies obtained from the MC simulations are given in Fig. 16, while the corresponding expectation value ($<E_Q>$) derived from the partition function (Eq. (12)) becomes as follows:

$$<E_Q>=E_H<n>+E_0+\frac{1}{2}<E^O>, \quad (15)$$

where

$$<E^O>=\sum_j^{5M}\left[\frac{h\nu_j}{2}+\frac{h\nu_j}{\exp\{h\nu_j/(k_BT)\}-1}\right]. \quad (16)$$

The contribution from the kinetic energy terms is subtracted in Eq. 15. It is impossible to estimate the intermolecular vibration frequencies (ν) from the MC simulations. Therefore, we simply assumed that the vibrational frequency for the translation and libration modes are 145 and 569 cm^{-1}, respectively, at a density of 1.0 g cm^{-3}.[24] E_H, E_0 and the vibrational frequencies may depend on the density of the system. E_H and E_0 are represented by a quadratic function of the density of the liquid (ρ), the Grüneisen's approximation[25] is applied to the vibrational frequencies:

$$\frac{\mathrm{d}\ln\nu_j}{\mathrm{d}V}=-\frac{\gamma}{V}. \quad (17)$$

The parameters were determined by a least-squares fit of

Eq. 15, while referring to the configuration energies obtained by the MC simulations. E_H, E_0 and the Grüneissen's γ were obtained as

$$E_H = 0.296\,(\rho + 2.65)^2 - 14.2,$$
$$E_0/M = 3.47\,(\rho - 2.00)^2 - 23.5,$$

and

$$\gamma = 0.33, \tag{18}$$

where the units of the energy and the density are kJ mol^{-1} and g cm^{-3}, respectively.

E_H was calculated to be -10.3 kJ mol^{-1} at a density of 1.0 g cm^{-3}. This energy is surprisingly small compared with the hydrogen bonding energy of the HF dimer in the gas phase, which was estimated to be -20.9 ± 6.3 kJ mol^{-1}.[15] The intrinsic hydrogen bond energy is considered to be split into two parts (E_H and E_0) in our treatment. E_H measures the energy associated with the formation or breaking of a hydrogen bond in the liquid phase, but does not a measure of the intrinsic hydrogen bonding energy. We can also estimate E_H from the bonding energy distribution function. As discussed in the section concerning the hydrogen bonding structure, the bonding distribution function is regarded as being a superposition of three Gaussian-type distributions of molecules which have one, two and three hydrogen bonds. The energy differences between the centers of the distributions correspond to the energy per one hydrogen bond in the liquid phase (Fig. 11). It is estimated to be about 12 kJ mol^{-1}, which is comparable with the E_H obtained here.

Next, the distribution function of n was calculated by MC simulations using a threshold pair energy of -10.0 kJ mol^{-1} (Fig. 17), while that derived from the partition function became

$$P_n = \exp(an^2 + bn)\cdot\exp\{-E_H\cdot n/(k_BT)\}/Z^H(M, T, V) \tag{19}$$

By a least-squares fit of the function, the parameters of the density of states were obtained to be -0.0270 and 1.93 for a and b, respectively. The distribution function of n is well represented by Eq. 19 (Fig. 17). This rationalizes the functional form (Eq. 8) for the density of states.

Thermodynamic Properties. In this section we evaluate the thermodynamic properties of liquid HF using the partition function. Before presenting discussion concerning each thermodynamic property, the average number of hydrogen bonds ($\langle n\rangle$) is discussed, since it is a fundamental quantity in our model. $\langle n\rangle$ is given as

$$\begin{aligned}\langle n\rangle &= \int_0^{n_{max}} n\cdot\exp(an^2 + bn)\cdot\exp\{-E_H\cdot n/(k_BT)\}dn/Z^H \\ &= \int_\chi^{\chi+n_{max}} (t-\chi)\exp(at^2)dt/Z^H \\ &= -\chi + \frac{1}{2a}\frac{\partial \ln A(\chi)}{\partial\chi}.\end{aligned} \tag{20}$$

Thus $\langle n\rangle$ at 273 K and at a density of 1.0 g cm^{-3} was calculated to be 118, which compares to 119 obtained directly from the MC simulations and 108 obtained through an analysis of the bonding energy distribution functions (the section concerning the hydrogen bonding structure).

When the range of the integral of Eq. 20 is sufficiently large to cover the entire integrand, and the integration is performed from $-\infty$ to $+\infty$, $\langle n\rangle$ becomes simply

$$\langle n\rangle = -\frac{b - E_H/(k_BT)}{2a}. \tag{21}$$

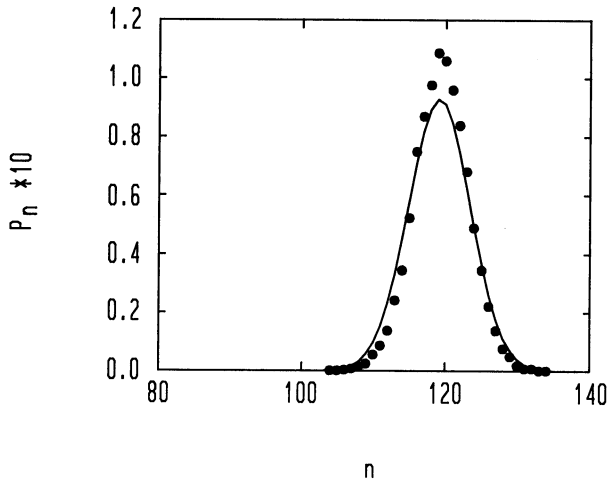

Fig. 17. Distribution function of n at a temperature of 273 K and a density of 1.0 g cm^{-3}. The solid line indicates the calculation by Eq. 19 and the circles were obtained by a Monte Carlo simulation.

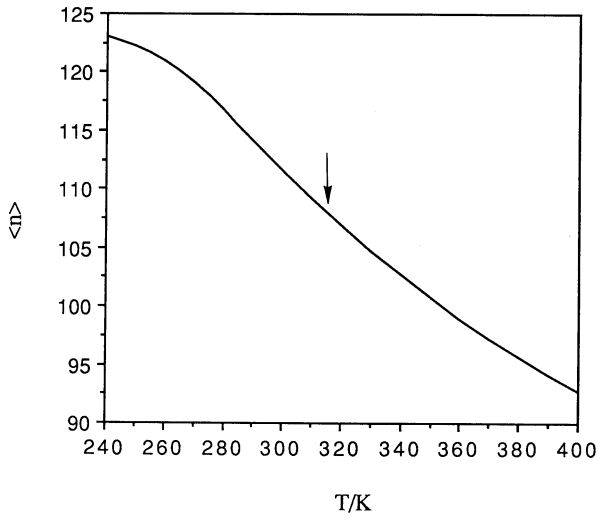

Fig. 18. Temperature dependence of the averaged number of hydrogen bonds in a 125 molecular system at a density of 1.0 g cm^{-3}. The arrow indicates the point of inflection.

Namely, $<n>$ decreases in proportion to $1/T$. This is the case of liquid water,[18] but not the case of liquid HF. The difference is due to the fact that the hydrogen bonds in liquid water are considerably broken, i.e., $<n>$ is only about 58% of n_{max} at 300 K, whereas the bonds are not broken so much in liquid HF, i.e., $<n>$ is 95% of n_{max} at 273 K. The temperature dependence of $<n>$ is shown in Fig. 18. There is a point of inflection at the temperature where $<n>$ is about 106. In both the low- and high-temperature regions the second term of Eq. 20 contributes and the rate of change becomes small as either $<n>$ approaches to it maximum (n_{max}) or to it minimum (zero).

i) Heat Capacity at Constant Volume: The heat capacity at constant volume (C_V) is given as

$$C_V=\left(\frac{\partial<E>}{\partial T}\right)_V=\frac{N}{M}(C_V^{H}+C_V^{O}) \tag{22}$$

$$C_V^{H}=E_H\frac{\partial<n>}{\partial T}$$

$$=-\frac{E_H^2}{2ak_BT^2}\left\{-\frac{1}{2a}\frac{\partial^2\ln A(\chi)}{\partial\chi^2}+1\right\}, \tag{23}$$

and

$$C_V^{O}=k_B\sum_j^{5M}\frac{\exp\{h\nu_j/(k_BT)\}}{[\exp\{h\nu_j/(k_BT)\}-1]^2}\{h\nu_j/(k_BT)\}^2. \tag{24}$$

where C_V^{H} and C_V^{O} are the contributions of the heat capacity from the hydrogen bond and the harmonic oscillator terms. From Eq. 22, C_V is calculated to be 50.8 J K^{-1} mol^{-1} at 273 K and at 0.1 MPa. It is compared with the experimental value[2] of 42.8 J K^{-1} mol^{-1}. C_V of liquid HF is larger than that of simple liquids. The contribution from the H-bond term, the first term of Eq. 22, is responsible for the large C_V of the hydrogen bonded liquids.

The temperature dependence of C_V at 0.1 MPa shown in Fig. 19 along with the experimental values. C_V of liquid HF increases with an increase of the temperature. The temperature dependence is quite different from that of water.[26] Namely, C_V of liquid water decreases as the temperature rises. To understand the hydrogen bond effect on C_V, we concentrate on C_V^{H}; C_V^{H} is proportional to the derivative of $<n>$ with respect to the temperature. (Refer to the discussions concerning $<n>$ given above.) From Eq. 21, C_V^{H} of liquid water is

$$\frac{N}{M}C_V^{H}=-\frac{N}{M}\frac{E_H^2}{2ak_BT^2} \tag{25}$$

This equation clearly shows that C_V^{H} decreases with an increase in the temperature. On the other hand, C_V^{H} of liquid HF becomes larger as the temperature rises in low temperature region, and reaches it maximum at the point of inflection. Since the temperature of liquid HF corresponds to the low temperature region of $<n>$, the effect of hydrogen bonds on C_V is opposite to that of liquid water.

ii) Equation of State: The pressure of the system (P) is

$$P=-\left(\frac{\partial F}{\partial V}\right)_T$$

$$=\frac{N}{M}\left(-<n>\frac{\partial E_H}{\partial V}-\frac{\partial E_0}{\partial V}+\gamma\frac{<E^{O}>}{V}\right). \tag{26}$$

where $<E^{O}>$ is the average energy of the harmonic oscillators (Eq. 16). The p-ρ projection of the equation

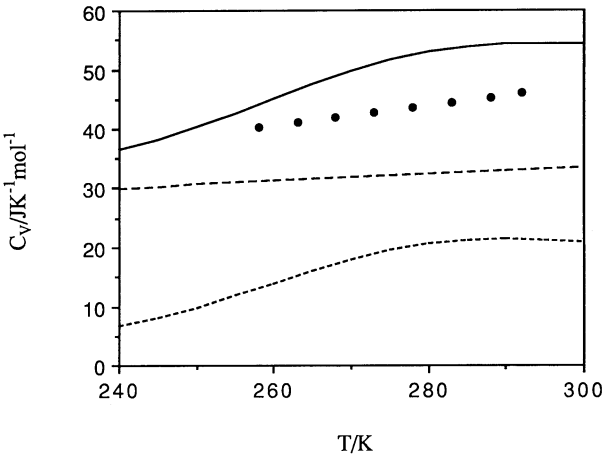

Fig. 19. Temperature dependence of the heat capacity at constant volume, C_V, at 0.1 MPa. —: from the partition function, ·····: from the hydrogen bond term, ----: from the harmonic oscillator term, ●: experimental data. (Ref. 2).

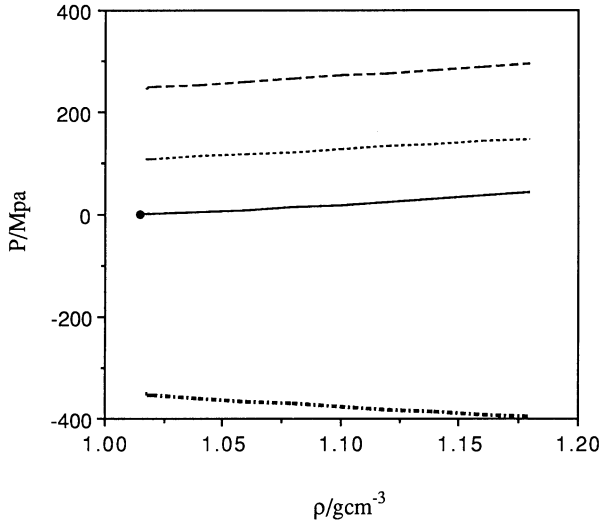

Fig. 20. Pressure versus density at a temperature of 273 K. —: from the partition function, ·····: from the hydrogen bond term, ----: from the harmonic oscillator term, -·-·-: from the background potential term. ●: experimental data. (Ref. 27).

of state for liquid HF is shown in Fig. 20, along with the contributions from the three terms: the H-bond, the background potential and the harmonic oscillator term. The density of liquid HF at 273 K under the atmosphere was calculated to be 1.02 g cm^{-3}, which compares well with the experimental value[27] of 1.02 g cm^{-3} (Fig. 20). Among the three components, the H-bond and the harmonic oscillator term contribute to a positive pressure, while the background term contributes to a negative pressure. The balance of the former and the later determines the volume of the system. The same tendency has been pointed out regarding liquid water using a similar partition function.[18] The contribution of the H-bond term to the pressure of the system is considerably larger in liquid HF than in liquid water. This suggests that the volume of liquid HF is considerably expanded by the effect of hydrogen bonds.

The calculated densities of the liquid are in good agreement with the experiment over the entire range of temperature of liquid (Fig. 21).

iii) Isothermal Compressibility: The isothermal compressibility (κ_T) becomes

$$\kappa_T = -\frac{1}{V}\left(\frac{\partial V}{\partial P}\right)_T = \frac{1}{-\frac{N}{M}V\left(-\langle n\rangle\frac{\partial^2 E_H}{\partial V^2} - \frac{\partial\langle n\rangle}{\partial V}\frac{\partial E_H}{\partial V} - \frac{\partial^2 E_0}{\partial V^2} + \frac{\gamma^2 C_V^{\circ} T - \langle E^{\circ}\rangle(\gamma+\gamma^2)}{V^2}\right)}. \quad (27)$$

where

$$\frac{N}{M}\frac{\partial\langle n\rangle}{\partial V} = -\frac{C_V^{H} T}{E_H^2}\frac{\partial E_H}{\partial V}. \quad (28)$$

κ_T is plotted against the temperature in Fig. 22 along with

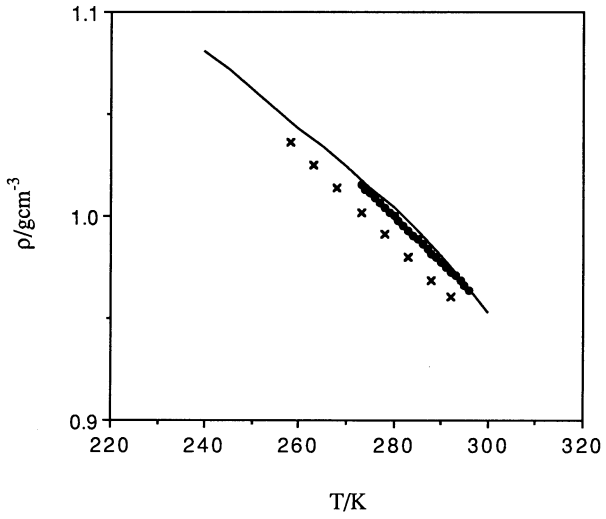

Fig. 21. Temperature dependence of the density of HF liquid. —: calculated from the partition function, ●: experiment (Ref. 27), ×: experiment. (Ref. 29).

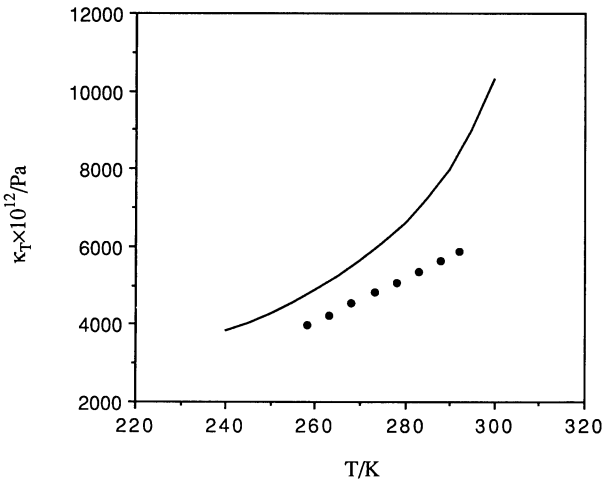

Fig. 22. Temperature dependence of the isothermal compressibility (κ_T). —: from the partition function, ●: experiment. (Ref. 2)

experiments. The calculated κ_T well compare with the experimental values. Unlike liquid water, κ_T of liquid HF increases monotonically as the temperature rises. κ_T has been observed to be 4818×10^{-12} Pa^{-1} at 273 K and at 0.1 MPa.[2] It is very large compared to that of nonpolar liquids whose κ_T is about 1000×10^{-12} Pa^{-1}.[28] The calculation reproduced the large κ_T of luquid HF successfully. The density of liquid HF (1.0 g cm^{-3}) is very small compared to that of a solid[23] (1.6 g cm^{-3}). The effects of hydrogen bonds work to expand the volume of liquid HF, as pointed out in ii). The low density may be responsible for the large κ_T of the liquid, as well as for the direct effect appearing in the first two terms of the denominator in Eq. 27.

iv) Coefficient of Thermal Expansion: The coefficient of thermal expansion (α_P) is written as

$$\alpha_P = -\frac{1}{V}\left(\frac{\partial V}{\partial T}\right)_P = \frac{N}{M}\left(-\frac{\partial\langle n\rangle}{\partial T}\frac{\partial E_H}{\partial V} + \gamma\frac{C_V^{\circ}}{V}\right)\kappa_T, \quad (29)$$

where

$$\frac{N}{M}\frac{\partial\langle n\rangle}{\partial T} = \frac{C_V^{H}}{E_H}, \quad (30)$$

The calculated α_P is give in Fig. 23. The calculation somewhat stresses the temperature dependence. It is known that α_P of liquid water becomes negative at low temperature.[26] For liquid water, we could show that the first negative term of Eq. 29 becomes larger in magnitude than that of the second positive term at low temperature, while the negative term, especially $d\langle n\rangle/dT$, is too small to overcome the positive term in liquid HF. Thus, α_P of liquid HF remains positive in the

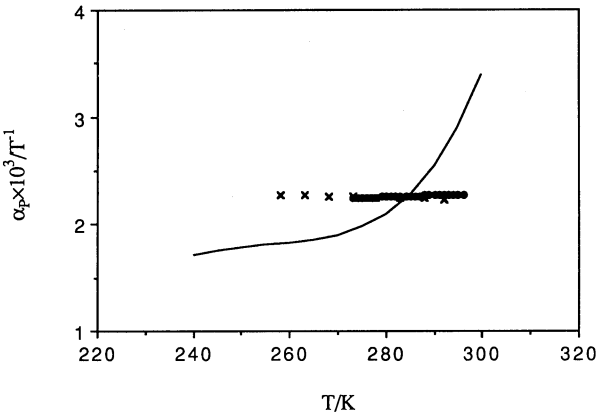

Fig. 23. Temperature dependence of the thermal expansion coefficient (α_P). —: from the partition function, ●: estimated from experimental data of density (Ref. 28), ×: experiment. (Ref. 2)

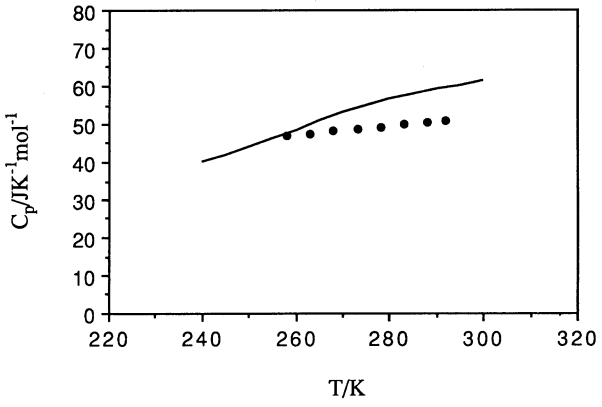

Fig. 24. Temperature dependence of the heat capacity at constant pressure (c_P). —: from the partition function, ●: experiment. (Ref. 30)

temperature range of the liquid.

v) Heat Capacity at Constant Pressure: The heat capacity at constant pressure (C_P) was calculated using C_V, κ_T, and α_P:

$$C_P = C_V + \frac{\alpha_P^2 VT}{\kappa_T} \tag{31}$$

Figure 24 shows the temperature dependence of C_P along with the experimental values. The calculations reproduced the experimental values satisfactorily.

Concluding Remarks

We generated a new type of intermolecular potential function for HF molecules. It reproduces the *ab initio* interaction energies of the HF dimer to reasonable accuracy over a wide range of potential energy surfaces.

The MC simulations using the present potential function revealed that the bonding energy distribution function has three peaks. Detailed analyses of the distribution function and the hydrogen bonding structures revealed that there are three different environments of molecules in the liquid: molecules having one, two and three hydrogen bonds with neighbors. Since the statistical property may depend on the potential function used in the simulations, it is safe to say that this is true in liquid of 'STO-3G HF'. To ascertain whether this is true or not in real liquid HF, a more accurate potential function may be required. In any case, as far as we know, the multiplet has been known only for liquid alcohols and our observation is only the second one.

A partition function of liquid HF was derived and the thermodynamic properties were evaluated from it. The calculated thermodynamic properties compared well with the experimental values. Moreover, we have shed some light on the effects of hydrogen bonds on each thermodynamic property, and have compared them with those of liquid water based on the partition function. The hydrogen bonds are considerably broken in liquid water, while those of liquid HF are not broken very much. This results in the different features of hydrogen bonding effects on the thermodynamic properties of these liquids.

There remain some difficulties concerning how to estimate the parameters involved in our partition function. Especially, it is impossible to estimate the intermolecular vibrational frequencies of the harmonic oscillators using the MC simulations. A recently developed quenching technique[31,32] will be helpful in evaluating the parameters of our partition function, since the structures and potential energies at the local minima and intermolecular vibrational frequencies will become available. However, this will be practically very difficult for quite some time, since it requires a huge amount of computer time.

Numerical calculations were partly carried out at the Computer Center of the Institute for Molecular Science. This work was supported by a Grant-in-Aid for Science Research on Priority Areas from the Ministry of Education, Science and Culture.

References

1) T. R. Dyke and J. S. Muenter, *J. Chem. Phys.*, **60**, 2929 (1974).
2) R. T. Lagemann and C. H. Knowles, *J. Chem. Phys.*, **32**, 561 (1960).
3) M. L. Klein and I. R. McDonald, *J. Chem. Phys.*, **71**, 298 (1979).
4) W. L. Jorgensen, *J. Am. Chem. Soc.*, **100**, 7824 (1978).
5) W. L. Jorgensen, *J. Chem. Phys.*, **70**, 5888 (1979).
6) M. E. Cournoyer and W. L. Jorgensen, *Mol. Phys.*, **51**, 119 (1984).
7) F. H. Stillinger and A. Rahman, *J. Chem. Phys.*, **60**, 1545 (1974).
8) O. Matsuoka, E. Clementi, and M. Yoshimine, *J. Chem. Phys.*, **64**, 1351 (1976); V. Carravetta and E. Clementi, *J. Chem. Phys.*, **81**, 2646 (1984); G. C. Lie and E. Clementi, *Phys. Rev. A,*

33, 2679 (1986).
9) K. Honda and K. Kitaura, *Chem. Phys. Lett.*, **140**, 53 (1987).
10) K. Kitaura and K. Morokuma, *Int. J. Quantum Chem.*, **10**, 325 (1976).
11) G. Némethy and H. A. Scheraga, *J. Chem. Phys.*, **36**, 3382 (1962); A. Ben-Naim, "Water and Aqueous Solutions," Plenum, New York (1974).
12) W. L. Jorgensen, *J. Am. Chem. Soc.*, **102**, 543 (1980); W. L. Jorgensen, *J. Phys. Chem.*, **90**, 1276 (1986).
13) J. M. Foster and S. F. Boys, *Rev. Mod. Phys.*, **32**, 300 (1960).
14) T. R. Dyke, B. J. Howard, and W. Klemperer, *J. Chem. Phys.*, **56**, 2442 (1972).
15) G. H. F. Diercksen and W. P. Kraemer, *Chem. Phys. Lett.*, **6**, 419 (1970).
16) N. Metropolis, A. W. Rosenbluth, M. N. Rosenbluth, A. H. Teller, and E. Teller, *J. Chem. Phys.*, **21**, 1087 (1953).
17) D. Levesque, J.J. Weis, and J. P. Hansen, in "Applications of the Monte Carlo Method in Statistical Physics," ed by K. Binder, Springer-Verlag, Berlin (1987), p. 37.
18) K. Honda, K. Kitaura, and K. Nishimoto, *Mol. Simul.*, **6**, 275 (1991).
19) J. A. Pople, *Proc. R. Soc. London, Ser. A*, **205**, 163 (1951).
20) A. Rice and M. G. Sceats, *J. Phys. Chem.*, **85**, 1108 (1981).
21) O. Weres and S. A. Rice, *J. Am. Chem. Soc.*, **94**, 8983 (1972).
22) H.E. Stanley and J. Teixeira, *J. Chem. Phys.*, **73**, 3404 (1980)
23) M. Atoji and W. N. Lipscomb, *Acta Crystallogr.*, **7**, 173 (1954); M. W. Johnson, E. Sánder and E. Arzi, *Acta Crystallogr., Sect. B*, **31**, 1998 (1975).
24) P. V. Huong, J. C. Cornut, and B. Desbat, *J. Chem. Phys.*, **77**, 5406 (1982).
25) R. Kubo, "Statistical Mechanics," North-Holland, Amsterdam (1988), p. 136; J. W. Shaner, *J. Chem. Phys.*, **89**, 1616 (1988); J. Belak, R. D. Etters, and R. LeSar, *J. Chem. Phys.*, **89**, 1625 (1988).
26) D. Eisenberg and W. Kauzmann, "The Structure and Properties of Water," Oxford University, New York (1969).
27) I. Sheft, A. J. Perkins, and H. H. Hymsn, *J. Inorg. Nucl. Chem.*, **35**, 3677 (1973).
28) Y. Marcus, "Introduction to Liquid State Chemistry," John Wiley & Sons, London (1977).
29) J. H. Simons and J. W. Bouknight, *J. Am. Chem. Soc.*, **54**, 129 (1932).
30) J-H. Hu, D. White, and H. L. Johnston, *J. Am. Chem. Soc.*, **75**, 1232 (1953).
31) A. Pohorille, L. R. Pratt, R. A. LaViolette, M. A. Wilson, and R. D. MacElroy, *J. Chem. Phys.*, **87**, 6070 (1987).
32) I. Ohmine, H. Tanaka, and P. G. Wolynes, *J. Chem. Phys.*, **89**, 5852 (1988).